1521-0103/344/1/113–123$25.00
THE JOURNAL OF PHARMACOLOGY AND EXPERIMENTAL THERAPEUTICS

http://dx.doi.org/10.1124/jpet.112.197905
J Pharmacol Exp Ther 344:113–123, January 2013

Functional and Structural Interaction of (−)-Reboxetine with the Human $\alpha4\beta2$ Nicotinic Acetylcholine Receptor

Hugo R. Arias, Nikolai B. Fedorov, Lisa C. Benson, Patrick M. Lippiello, Greg J. Gatto, Dominik Feuerbach, and Marcelo O. Ortells

Department of Medical Education, College of Medicine, California Northstate University, Elk Grove, California (H.R.A); Preclinical Research, Targacept, Inc., Winston Salem, North Carolina (N.B.F., L.C.B., P.M.L., G.J.G.); Neuroscience Research, Novartis Institutes for Biomedical Research, Basel, Switzerland (D.F., M.O.O.); and Faculty of Medicine (D.F.) and CONICET (M.O.O.), University of Morón, Argentina

Received June 28, 2012; accepted September 25, 2012

ABSTRACT

The interaction of the selective norepinephrine reuptake inhibitor (−)-reboxetine with the human $\alpha4\beta2$ nicotinic acetylcholine receptor (nAChR) in different conformational states was studied by several functional and structural approaches. Patch-clamp and Ca^{2+}-influx results indicate that (−)-reboxetine does not activate h$\alpha4\beta2$ nAChRs via interaction with the orthosteric sites, but inhibits agonist-induced h$\alpha4\beta2$ activation by a noncompetitive mechanism. Consistently, the results from the electrophysiology-based functional approach suggest that (−)-reboxetine may act via open channel block; therefore, it is capable of producing a use-dependent type of inhibition of the h$\alpha4\beta2$ nAChR function. We tested whether (−)-reboxetine binds to the luminal [^{3}H]imipramine site. The results indicate that, although (−)-reboxetine binds with low affinity to this site, it discriminates between the resting and desensitized h$\alpha4\beta2$ nAChR ion channels. Patch-clamp results also indicate that (−)-reboxetine progressively inhibits the h$\alpha4\beta2$ nAChR with two-fold higher potency at the end of one-second application of agonist, compared with the peak current. The molecular docking studies show that (−)-reboxetine blocks the ion channel at the level of the imipramine locus, between M2 rings 6′ and 14′. In addition, we found a (−)-reboxetine conformer that docks in the helix bundle of the $\alpha4$ subunit, near the middle region. According to molecular dynamics simulations, (−)-reboxetine binding is stable for both sites, albeit less stable than imipramine. The interaction of these drugs with the helix bundle might alter allostericaly the functionality of the channel. In conclusion, the clinical action of (−)-reboxetine may be produced (at least partially) by its inhibitory action on h$\alpha4\beta2$ nAChRs.

Introduction

Selective norepinephrine reuptake inhibitors (SNRIs) have been used with great success to treat the symptoms of depressive disorders and other related neuropsychiatric illnesses, including panic attacks, narcolepsy, and attention deficit hyperactivity disorder (reviewed in Gorman and Kent, 1999). Structurally, SNRIs can be classified as secondary amine tricyclic antidepressants (e.g., desipramine) and non-tricyclic antidepressants (e.g., reboxetine). Reboxetine, a racemate of (−)-*R,R*- and (+)-(*S,S*)-([2-[α[2-ethoxyphenoxy]benzyl]-morpholine], is the first commercially available SNRI developed specifically as a first-line therapy for depressive disorders (Hajos et al., 2004). Although reboxetine is currently in use in several European countries, it has not been approved by the Food and Drug Administration for use in the United States.

From the mechanistic point of view, SNRIs inhibit norepinephrine reuptake transporters, increasing the synaptic concentration of norepinephrine, thereby enhancing the activity of postsynaptic norepinephrine receptors (Hajos et al., 2004). Nevertheless, SNRIs also behave as noncompetitive antagonists (NCAs) of several nicotinic acetylcholine receptors (nAChRs) (Hennings et al., 1999; Izaguirre et al., 1997; Miller et al., 2002; Rana et al., 1993; reviewed in Arias et al., 2006). nAChRs are members of the Cys-loop ligand-gated ion channel superfamily, which also includes types A and C γ-aminobutyric acid, type 3 serotonin, and glycine receptors (reviewed in Arias et al., 2006; Arias, 2010; Albuquerque et al., 2009). The antidepressant-induced inhibition of one or more nAChR subtypes might be related to their therapeutic actions. This is in agreement with the cholinergic-adrenergic hypothesis, which states that the hyperactivity or hypersensitivity of the cholinergic system over the adrenergic system can lead to depressed mood states (reviewed in Shytle et al., 2002). This hypothesis is also supported by epidemiologic results showing a higher rate of smoking in depressed patients than in the general population (reviewed in Picciotto et al., 2002) and by animal behavior studies indicating that nicotinic agonists enhance the antidepressant activity of reboxetine (Andreasen et al., 2011).

This research was supported by grants from the Consejo Nacional de Investigaciones Científicas y Técnicas (to M.O.).
dx.doi.org/10.1124/jpet.112.197905.

ABBREVIATIONS: ACh, acetylcholine; BS, binding saline; BTx, κ-bungarotoxin; CCh, carbamylcholine; IC_{50}, ligand concentration that inhibits 50% binding or ion flux; K_d, dissociation constant; K_i, inhibition constant; nAChR, nicotinic acetylcholine receptor; NCA, noncompetitive antagonist; n_H, Hill coefficient; (−)-reboxetine, (−)-R,R-([2-[α[2-ethoxyphenoxy]benzyl]-morpholine]); κ- RT, room temperature; SNRI, selective norepinephrine reuptake inhibitor.

Considering these results, neuronal nAChRs could be potential targets for enhancing the beneficial actions elicited by SNRIs. An interesting example is the attenuation of nicotine self-administration in rats elicited by reboxetine (Rauhut et al., 2002) and desipramine (Paterson et al., 2008), supporting a potential therapeutic use of these antidepressants for the treatment of nicotine addiction. Thus, a better understanding of the interaction of SNRIs with different nAChR subtypes is crucial to the development of new and safer antidepressant therapies or even for novel clinical uses. In this regard, we have characterized the interaction of (−)-reboxetine with the human (h) $\alpha4\beta2$ nAChR, the most abundant nAChR subtype in the brain, in different conformational states. To accomplish this, we used structural and functional approaches, including radioligand binding assays using the noncompetitive antagonist [^{3}H]imipramine and the agonist [^{3}H]cytisine, Ca^{2+}-influx and patch-clamp measurements, and molecular docking and dynamics studies.

Materials and Methods

Materials. [^{3}H]Imipramine hydrochloride (47.5 Ci/mmol) and [^{3}H]cytisine hydrochloride (35.6 Ci/mmol) were obtained from PerkinElmer Life Sciences Products, Inc. (Boston, MA) and stored at -20°C. (−)-Reboxetine mesylate, acetylcholine chloride (ACh), imipramine hydrochloride, carbamylcholine chloride (CCh), pepstatin A, leupeptin, aprotinin, benzamidine, phenylmethylsulfonyl fluoride, and polyethylenimine were purchased from Sigma-Aldrich (St. Louis, MO). Geneticin (G418) and hygromycine B and (±)-epibatidine were obtained from Tocris Bioscience (Ellisville, MO). k-Bungarotoxin (k-BTx) was obtained from Biotoxins Incorporated (St. Cloud, FL). Fetal bovine serum and trypsin/EDTA were purchased form Gibco BRL (Paisley, UK). Salts were of analytical grade.

Ca^{2+} Influx Measurements in HEK293-h$\alpha4\beta2$ Cells. Ca^{2+} influx experiments were performed using the HEK293-h$\alpha4\beta2$ cell line, which was cultured as explained previously (Arias et al., 2010b; Arias, 2010). In brief, cells were cultured in a 1:1 mixture of Dulbecco's modified Eagle medium containing 3.7 g/l $NaHCO_3$, 1.0 g/l sucrose, supplemented with stable glutamine (L-AlanyL-L-Glutamine, 524 mg/l), and Ham's F-12 Nutrient Mixture containing 1.176 g/l $NaHCO_3$ and supplemented with 10% (v/v) fetal bovine serum, Geneticin (G418; 0.2 mg/ml), and hygromycine B (0.2 mg/ml). The cells were maintained at 37°C, 5% CO_2, and 95% relative humidity and were passaged every 3 days by detaching the cells from the cell culture flask by washing with phosphate-buffered saline and brief incubation (~3 minutes) with trypsin (0.5 mg/ml)/EDTA (0.2 mg/ml). After cell culturing, 5×10^4 cells per well were seeded 48 hours before the Ca^{2+} influx experiment on black poly-L-lysine 96-well plates (Costar, Corning Inc., New York) and incubated at 37°C in a humidified atmosphere (5% CO_2/95% air), as previously described (Arias et al., 2010b; Arias, 2010; Michelmore et al., 2002). Sixteen hours before the experiment, the medium was changed to 1% bovine serum albumin (BSA) in HEPES-buffered salt solution (HBSS) (130 mM NaCl, 5.4 mM KCl, 2 mM $CaCl_2$, 0.8 mM $MgSO_4$, 0.9 mM NaH_2PO_4, 25 mM glucose, 20 mM HEPES; pH, 7.4). On the day of the experiment, the medium was removed by flicking the plates and replaced with 100 µl HBSS/1% BSA containing 2 µM Fluo-4 (Molecular Probes, Eugene, OR) in the presence of 2.5 mM probenecid (Sigma, Buchs, Switzerland). The cells were then incubated at 37°C in a humidified atmosphere (5% CO_2/95% air) for 1 hour. Plates were flicked to remove excess of Fluo-4, washed twice with HBSS/1% BSA, and finally refilled with 100 µl of HBSS containing different concentrations of (−)-reboxetine and were preincubated for 5 minutes. Plates were then placed in the cell plate stage of the fluorimetric imaging plate reader (FLIPR, PC, Molecular Devices, Sunnyvale, CA). A baseline consisting of 5 measurements of 0.4 seconds each was recorded. (±)-Epibatidine (0.1 µM) was then added from the agonist plate to the cell plate using the 96-tip pipettor simultaneously to fluorescence recordings for a total length of 3 minutes. The laser excitation and emission wavelengths were 488 and 510 nm, at 1 W, with a CCD camera opening of 0.4 seconds.

A 1:1 ratio of the alpha4 and the beta2 gene was used for the generation of the HEK293-human nAChRalpha4beta2 cell line. Experiments were conducted at 37°C. The stoichiometries of $\alpha4\beta2$ in this experimental setting in HEK293 cells was 82% ($\alpha4_{(3)}\beta2_{(2)}$). The heterogeneous stoichiometry in the cell line results in a biphasic concentration response curve for acetylcholine in the calcium influx assay (Feuerbach et al., unpublished observations). The strong prevalence of the LS stoichiometry traps the existence of the much smaller amount of HS (18%), but in concentration response curves with a higher number of assessment points (e.g., 16 instead of 8), the HS fraction becomes evident. The stoichiometry of alpha4beta2 receptors have not been investigated as extensively in the SHEP cells as in the HEK293 cells. However, the EC50 and the nH value for ACh may suggest a higher percentage of HS, and the mixed population will be seen more easily.

Electrophysiological Measurements in SHEP1-h$\alpha4\beta2$ Cells. For electrophysiology-based assays, we used the subclonal human epithelial h$\alpha4\beta2$ cells (kindly provided by Dr. Ortrud Steinlein, Institute of Human Genetics, University Hospital, Ludwig-Maximilians-Universität, Munich, Germany) and subcloned pcDNA3.1-zeocin and pcDNA3.1-hygromycin vectors, respectively, into native nAChR-null SHEP1 cells to create the stably transfected, monoclonal subclonal human epithelial (SHEP1)-h$\alpha4\beta2$ cell line heterologously expressing h$\alpha4\beta2$ nAChRs. Cell cultures were maintained at low passage numbers (1–26 from frozen stocks to ensure the stable expression of the phenotype) in complete medium augmented with 0.5 mg/ml zeocin and 0.4 mg/ml hygromycin (to provide a positive selection of transfectants) and passaged once weekly by splitting the just-confluent cultures 1:50 to maintain cells in proliferative growth. Reverse-transcriptase polymerase chain reaction, immunofluorescence, radioligand-binding assays, and isotopic ion flux assays were conducted recurrently to confirm the stable expression of $\alpha4\beta2$ nAChRs as message, protein, ligand-binding sites, and functional receptors.

After removal from the incubator, the medium was aspirated, and the dissociation medium Accumax (ThermoFisher Scientific, Pittsburgh, PA) was added to the cells for 5 minutes. After the cells were lifted from the plate, new media was added and the cells were transferred to a 15 ml conical tube and centrifuged at 1000 rpm for 2 minutes. The supernatant was aspirated, and the cells were resuspended in 2 ml of external solution from which cells were placed in the Dynaflow chip mount on the stage of an inverted microscope (Carl Zeiss Inc., Thornwood, NY). On average, 5 minutes was necessary before the whole-cell recording configuration was established. To avoid modification of the cell conditions, a single cell was recorded per single load. To evoke fast responses (1 second), agonists were applied using a Dynaflow system (Cellectricon, Inc., Gaithersburg, MD), in which each channel delivered pressure-driven solutions at either 50 or 150 psi.

Conventional whole-cell current recordings, together with a computer-controlled Dynaflow system for fast application and removal of agonists, were used in these studies. In brief, the cells were placed in a silicon chip bath mount on an inverted Zeiss microscope. Cells chosen for analysis were continuously perfused with standard external solution. Glass microelectrodes 3–5 MΩ resistance were used to form tight seals (1 GΩ) on the cell surface until suction was applied to convert to conventional whole-cell recording. The cells were then voltage-clamped at holding potentials of −60 mV, and ion currents in response to application of ligands were measured. Whole-cell currents recorded with an Axon 700A amplifier were filtered at 1 kHz and sampled at 5 kHz by an ADC board 1440 (Molecular Devices, Sunnyvale, CA) and stored on the hard disk of a PC computer. Whole-cell access resistance was less than 20 MΩ. Whole-cell currents were acquired using a Clampex 10

(Molecular Devices Inc., San Diego, CA). Concentration-response profiles were fit and analyzed using Prism 5.0 (GraphPad Software Inc., San Diego, CA). The experimental data are presented as the mean ± S.E.M., and comparisons of different conditions were analyzed for statistical significance using Student's *t* tests. All experiments were performed at room temperature (RT; 22°C). More than 90% of the cells responded to ACh, and every cell presenting a measurable current was taken into account. All drugs were prepared daily from stock solutions.

For determination of potential agonist-like properties of (−)-reboxetine in this study, we first used 13 concentrations of ACh (0.1–1000 μM) to construct dose-response curves, followed by reboxetine (0.1–1000 μM). Then, one additional application of ACh (0.1–1000 μM) was performed to assure stability of responses or the existence of any residual inhibition and/or facilitation. To determine the extent of potential competitive types of inhibition, we applied five consecutive applications of 10 μM ACh (10 μM, 30-second intervals) and then preapplied (−)-reboxetine (3-200 μM, 2-second preapplication before coapplication) and measured peak current amplitude and the tail portion of the current. To determine the potential for non-competitive use-dependent inhibition, we used a procedure described by us and others previously (Fedorov et al., 2009; Giniatullin et al., 2000). In brief, 10 consecutive pulses of ACh (10 μM, 1-second duration with 30-second intervals) were applied to assure a stable baseline recording followed by 10 pulses of ACh in the presence of 1 or 10 μM (−)-reboxetine to induce use-dependent inhibition of responses by (−)-reboxetine, followed by application of ACh alone to evaluate recovery from inhibition.

The standard external solution contained 120 mM NaCl, 3 mM KCl, 2 mM $MgCl_2$, 2 mM $CaCl_2$, 25 mM D-glucose, and 10 mM HEPES and was adjusted to a pH of 7.4 with TRIS base. In the experiments, ACh was applied as an agonist without atropine, because our experimental data showed that 1 μM atropine sulfate did not affect ACh-induced currents (not shown) and because atropine itself has been reported to block nAChRs (Liu et al., 2008). For all conventional whole-cell recordings, TRIS electrodes were used and filled with solution containing 110 mM TRIS phosphate dibasic, 28 mM TRIS base, 11 mM EGTA, 2 mM $MgCl_2$, 0.1 mM $CaCl_2$, and 4 mM Mg-ATP (pH, 7.3). To initiate whole-cell current responses, ACh was delivered by moving cells from the control solution to agonist-containing solution and back so that solution exchange occurred within 50 milliseconds (based on 10%–90% peak current rise times). Intervals between drug applications (0.5–1 minutes) were adjusted specifically to ensure the stability of receptor responsiveness (without functional rundown), and the selection of pipette solutions used in most of the studies described here was made with the same objective.

Preparation of nAChR-Containing Membranes. To prepare cell membranes in large quantities, the method of Arias et al. (2010) was used. In brief, HEK293-hα4β2 cells were cultured separately in suspension using nontreated Petri dishes (150 mm × 15 mm). After culturing the cells for ~3 weeks, cells were harvested by gently scraping and were centrifuged at 1000 rpm for 5 minutes at 4°C using a Sorvall Super T21 centrifuge. Cells were resuspended in binding saline (BS) buffer (50 mM Tris-HCl, 120 mM NaCl, 5 mM KCl, 2 mM $CaCl_2$, 1 mM $MgCl_2$; pH, 7.4), containing 0.025% (w/v) sodium azide and a cocktail of protease inhibitors including, leupeptin, bacitracin, pepstatin A, aprotinin, benzamidine, and phenylmethylsulfonylfluoride. The suspension was maintained on ice and homogenized using a Polytron PT3000 (Brinkmann Instruments Inc., Westbury, NY), and then centrifuged at 10,000 rpm for 30 minutes at 4°C. The pellet was finally resuspended in BS buffer containing 20% sucrose (w/v) using the Polytron and briefly (6 × 15 s) sonicated (Branson Ultrasonics Co., Danbury, CT) to assure maximum homogenization. Total protein was determined using the bicinchoninic acid protein assay (ThermoFisher Scientific, Rockford, IL). The hα4β2 nAChR membrane preparation was stored at −80°C in 20% sucrose until required.

Radioligand Binding Experiments Using nAChRs in Different Conformational States. The effect of (−)-reboxetine on [^{3}H]imipramine and [^{3}H]cytisine binding to hα4β2 nAChRs in different conformational states was studied. In this regard, hα4β2 nAChR membranes (1.5 mg/ml) were suspended in BS buffer with 15 nM [^{3}H]imipramine in the presence of 0.1 μM (±)-epibatidine (desensitized/agonist-bound state) or 0.1 μM k-BTx (resting/k-BTx-bound state) or, alternatively, with 9.1 nM [^{3}H]cytisine in the absence of any ligand, and preincubated for 30 minutes at RT. k-BTx is a high-affinity competitive antagonist that maintains the nAChRs in the resting (closed) state (Moore and McCarthy, 1995). Nonspecific binding was determined in the presence of 100 μM imipramine ([^{3}H]imipramine experiments) and 1 mM CCh ([^{3}H]cytisine experiments).

The total volume was divided into aliquots, and increasing concentrations of the ligand under study were added to each tube and incubated for 2 hours at RT. nAChR-bound radioligand was then separated from free ligand by a filtration assay using a 48-sample harvester system with GF/B Whatman filters (Brandel Inc., Gaithersburg, MD), previously soaked with 0.5% polyethylenimine for 30 minutes. The membrane-containing filters were transferred to scintillation vials with 3 ml of Bio-Safe II (Research Product International Corp, Mount Prospect, IL), and the radioactivity was determined using a Beckman LS6500 scintillation counter (Beckman Coulter, Inc., Fullerton, CA).

The concentration-response data were curve-fitted by nonlinear least squares analysis using the Prism software. The corresponding IC_{50} values were calculated using the following equation:

$$\theta = 1/[l + ([L]/IC50)^{nH}] \quad (1)$$

where θ is the fractional amount of the radioligand bound in the presence of inhibitor at a concentration [L], compared with the amount of the radioligand bound in the absence of inhibitor (total binding). IC_{50} is the inhibitor concentration at which θ = 0.5 (50% bound), and n_H is the Hill coefficient. The observed IC_{50} values from the competition experiments described above were transformed into inhibition constant (K_i) values using the Cheng-Prusoff relationship (Cheng and Prusoff, 1973):

$$Ki = IC50/1 + ([[^3H]imipramine]/Kd^{imipramine}) \quad (2)$$

where [[^{3}H]imipramine] is the initial concentration of [^{3}H]imipramine and $K_d^{imipramine}$ corresponds to the inhibition constant of [^{3}H]imipramine (0.83 μM) (Arias et al., 2010b). The calculated K_i and n_H values are summarized in Table 2.

Molecular Docking of (−)-Reboxetine and Imipramine Within the hα4β2 nAChR Ion Channel. The neuronal hα4β2 nAChR was built by homology modeling using the electron microscopy structure of the *Torpedo* nAChR determined at ~4 Å resolution (PDB 2BG9) (Miyazawa et al., 2003; Unwin, 2005) as the template and using the programs Modeler 9.8 (Sali and Blundell, 1993) and SWIFT MODELER (Mathur et al., 2011). The hα4β2 nAChR structure was energy minimized using molecular mechanics using the program NAMD (Phillips et al., 2005), the CHARMM force field (Brooks et al., 2009), and the software VEGA ZZ as interface (Pedretti et al., 2004). The energy minimization was performed by fixing the backbone atoms to their original positions, to avoid distorting the secondary structure.

(−)-Reboxetine, in the protonated (P) and neutral (N) states, was first modeled using the VEGA ZZ program (Pedretti et al., 2004). Minimization and partial charge calculations were done using the MOPAC program as implemented in VEGA ZZ and using the semiempirical AM1 method. Subsequently, these molecules were docked into the nAChR ion channel using AutoDock Vina. The same protocol was used for imipramine.

The automatic docking procedure was used to investigate the binding modes of (−)-reboxetine, in the neutral and protonated states, and imipramine in the nAChR model of the whole receptor. The parameters used with AutoDock Vina were exhaustiveness of 570 and maximum number of modes of 20. Although the default and recommended value for the exhaustiveness parameter is eight, we used the maximum value that our computational system (an AMD ×6 six core processor computer with 8Gb RAM) allowed. Although the

software searched the whole receptor structure, the time used for each run was in the order of minutes. To achieve this performance, however, no flexible residues were allowed in the receptor models.

For each molecule [i.e., neutral and protonated (−)-reboxetine and imipramine], the program provides theoretical estimations of their affinities to the hα4β2 nAChR. The program gives the best 20 poses found for each run. However, before giving this final output, it performs an internal clustering in such a way that multiple similar results are trimmed. Nevertheless, in each output, several of the best 20 conformers are still superposed. From every cluster of superposed conformations, we selected the one with the highest binding affinity according to the Vina program. In this way, the number of binding sites found in every run is defined by the number of conformers remaining after this selection process.

To test the stability of (−)-reboxetine in their predicted docking sites, a 10-ns molecular dynamics was performed at 300K using the program NAMD, the CHARMM force field, and the software VEGA ZZ as interface. For comparison purposed, the same protocol was applied to imipramine. For this aim, the hα4β2 nAChR model was hydrated with a 10 Å minimum thick shell using the program solvate 1.0 (Grubmuller et al., 1996); this also added the appropriated number of Cl^- and Na^+ to neutralize the system, which was fully minimized using NAMD. During the molecular dynamics simulation and to reduce computation time, all residues and water molecules outside a 20 Å radius sphere and centered on the corresponding conformer were restricted to their original positions, whereas those within this sphere were free to move. The same size sphere was used to implement a spherical periodic boundary condition. To estimate the root mean square deviation (RMSD) (see Eq. 3) values with respect to the initial structure, the conformations during the simulation were extracted every 10-ps from the simulation trajectory of 10-ns total time.

$$\mathrm{RMSD} = \sqrt{\frac{\sum_{i=1}^{N} \partial_i^2}{N}} \qquad (3)$$

where N is the number of atoms from the ligand and ∂_i^2 is the distance between the corresponding ligand atoms obtained at each step and the starting conformation. RMSD values represent the inter-molecular conformational changes and the rotation and translation of the whole molecule. The RMSD was calculated using the program VEGA ZZ.

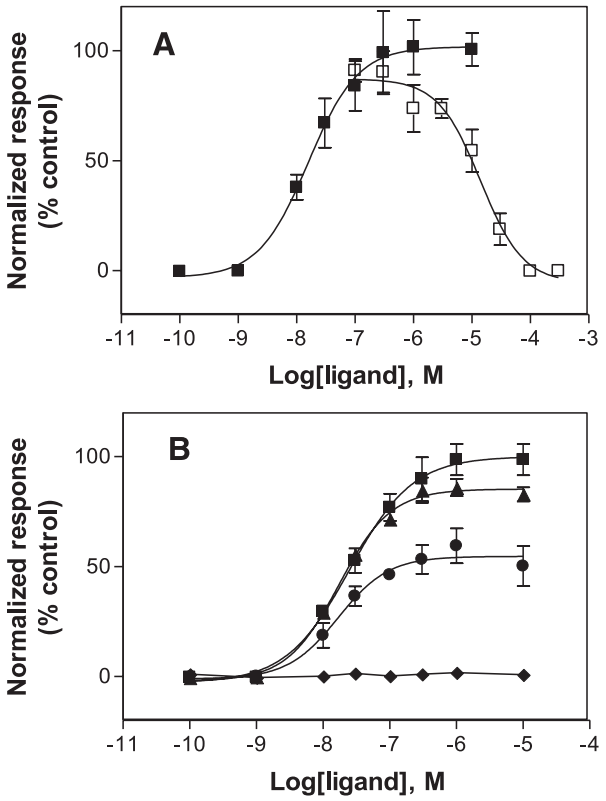

Fig. 1. (A) (−)-Reboxetine-induced inhibition of (±)-epibatidine–evoked calcium influx in HEK293-hα4β2 cells. The (±)-epibatidine–evoked calcium influx in HEK293-hα4β2 cells (■) was inhibited by preincubation (5 min) with several concentrations of (−)-reboxetine (□), followed by addition of 0.1 μM (±)-epibatidine. Response was normalized to the maximal (±)-epibatidine response, which was st as 100%. (B) Pretreatment with 1 (▲), 10 (●), or 100 (♦) μM (−)-reboxetine inhibits (±)-epibatidine–induced calcium influx in HEK293-hα4β2 cells in a dose-dependent and noncompetitive manner. The plots are representative of 28 (■), 6 (□), and 3 (▲, ●, ♦) determinations, respectively, where the error bars represent the S.D. values. The calculated IC_{50} and n_H values are summarized in Table 1.

Results

(−)-Reboxetine-Induced Inhibition of (±)-Epibatidine-Mediated Ca^{2+} Influx in HEK293-hα4β2 Cells. The potency of (±)-epibatidine to activate hα4β2 nAChRs was first determined by assessing the fluorescence change in HEK293-hα4β2 cells caused by an increase in intracellular Ca^{2+} after agonist stimulation (Fig. 1A). Increased concentrations of (±)-epibatidine activate the hα4β2 nAChR with potency EC_{50} = 30 ± 5 nM. The observed potency is in the same concentration range as that previously determined using cell lines expressing the same nAChR type (Arias et al., 2010b; Arias, 2010; Gerzanich et al., 1995). (±)-Epibatidine-induced nAChR activation is blocked by preincubation with (−)-reboxetine (Fig. 1A), with inhibitory potency IC_{50} = 16 ± 1 μM (Table 1). The fact that the n_H values for (−)-reboxetine are higher than unity (Table 1) indicates that the blocking process is produced in a cooperative manner. In turn, this suggests that (−)-reboxetine inhibits the nAChR by interacting with more than one binding site or that there are different inhibitory mechanisms. To determine the mechanism of inhibition elicited by (−)-reboxetine on the hα4β2 nAChR, different concentrations of (−)-reboxetine were added to one (±)-epibatidine concentration (Fig. 1B). The results indicate that (−)-reboxetine inhibits the hα4β2 nAChR in a dose-response manner and by a noncompetitive mechanism.

Lack of (−)-Reboxetine-Induced nAChR Activation Determined by Electrophysiology-Based Assays. To evaluate the ability of (−)-reboxetine to activate hα4β2 nAChRs, a wide range of (−)-reboxetine concentrations was applied to SHEP1-hα4β2 cells. The experimental design and results of these experiments are presented in Fig. 2. We initially applied ACh and followed this with an application of (−)-reboxetine and then one additional application of ACh (Fig. 2A). Under these experimental conditions, we were able to obtain a robust full dose response of ACh-induced hα4β2 nAChR activation (0.1–1000 μM; Fig. 2, B and C). Subsequent applications of (−)-reboxetine revealed no apparent current induction even at the highest concentrations used (1 mM; Fig. 2C). An additional application of ACh confirmed the presence of functional receptors with full recovery of the initial responses to ACh (Fig. 2, A and B). This result strongly suggests that (−)-reboxetine is not an agonist of α4β2 nAChRs (i.e., it does not interact with the orthosteric sites of the receptor).

(−)-Reboxetine Inhibits hα4β2 nAChR Function in a Dose-Dependent Manner. To determine whether (−)-reboxetine inhibis hα4β2 nAChR function, we first used

TABLE 1
Inhibitory potency (IC_{50}) of (−)-reboxetine for the hα4β2 nAChR

Method	Conformational State	IC_{50}	n_H[a]
		μM	
Ca^{2+} influx[b]			
5 min preincubation	Mix of activated and desensitized states	16.0 ± 1.0	1.45 ± 0.09
Patch clamp[c]			
Amplitude peak measurements	Mainly activated state	40.0 ± 0.7	1.10 ± 0.40
Tail current measurements, 2-s preincubation	Mainly desensitized state	21.0 ± 0.8	1.20 ± 0.30

[a] Hill coefficient.
[b,c] Values obtained from Fig. 1A[a] and Fig. 3[b], respectively.

a protocol of preapplication of (−)-reboxetine followed by co-application of a single concentration of ACh with increasing concentrations of (−)-reboxetine. In the first set of experiments, we used a concentration range of (−)-reboxetine from 0.001-1 μM (n = 3, not shown). In this concentration range, (−)-reboxetine did not produce significant inhibition of α4β2 receptor function. In the second set of experiments, we increased the concentration range of (−)-reboxetine to 0.3-200 μM (Fig. 3). In this case, (−)-reboxetine produced a robust inhibition of the hα4β2 nAChR function (Fig. 3A; Table 1). A relatively greater portion of the inhibitory action produced by (−)-reboxetine on hα4β2 nAChR function occurred at the end of the coapplication but not before that. As a result of this selective inhibition, the current kinetics was substantially modified by (−)-reboxetine. More specifically, the peak current amplitude (IC_{50} ~40 μM) was inhibited to a lesser extent than the steady-state (tail) currents (IC_{50} ~21 μM) at the final ACh application (Table 2). Changes in current kinetics consisted of a 3.2-fold increase in the rate of current decay, from τ = 0.47 seconds in controls to τ = 0.15 seconds in the presence of 200 μM (−)-reboxetine (Figs. 3C,D). Thus, our results indicate that the inhibition produced by (−)-reboxetine depends on the time of exposure, suggesting a time- and/or use-dependent mechanism of action via open-channel blockade. This pattern of functional changes resembles that recently published for AMPA-type glutamate receptors (Zaitsev et al., 2011). Therefore, the next question was to find out whether (−)-reboxetine produces open channel blockade.

(−)-Reboxetine Inhibits hα4β2 nAChR Function in a Use-Dependent Manner. To determine whether (−)-reboxetine inhibits hα4β2 nAChR function by an open-channel

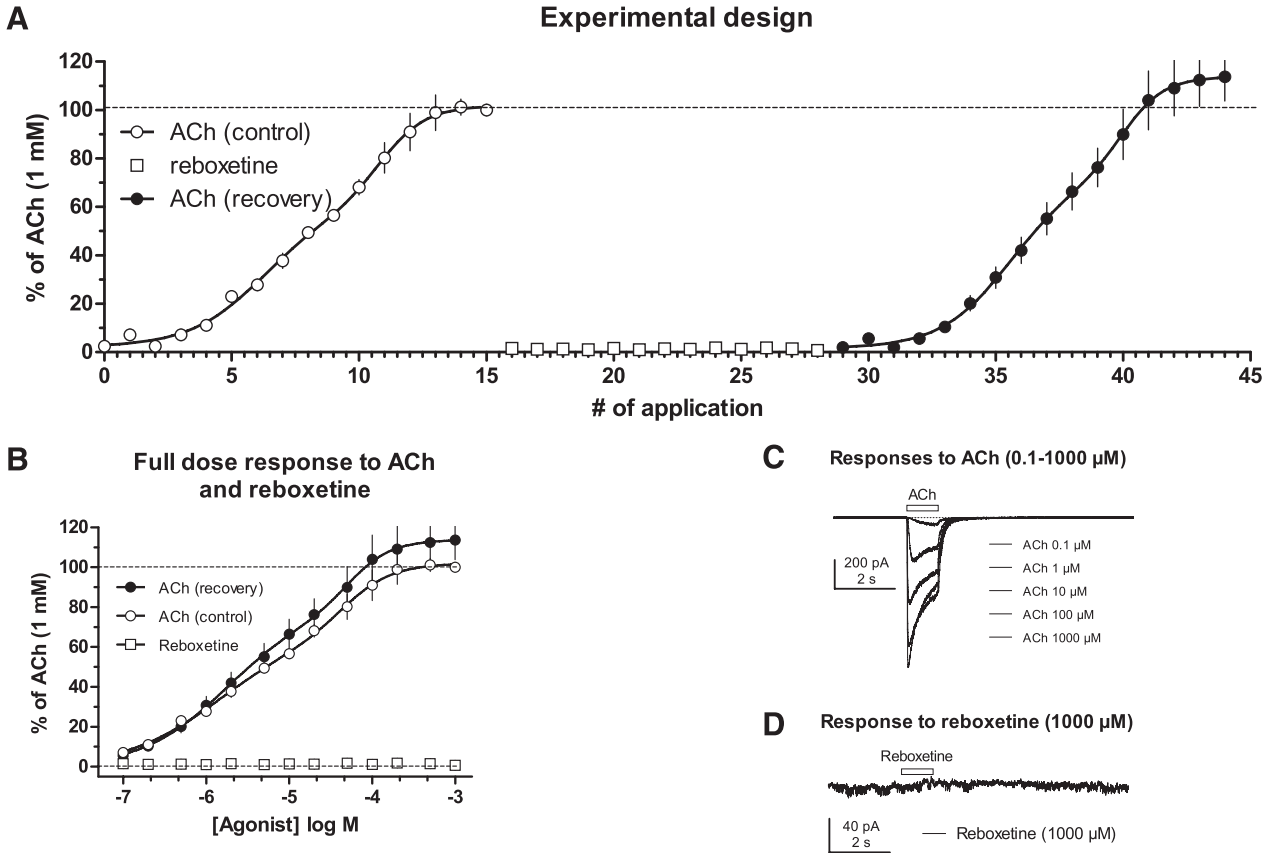

Fig. 2. (−)-Reboxetine does not activate hα4β2 nAChRs. (A) Plot representing the flow of experiments, with consecutive applications of increasing concentrations of ACh, starting with an ACh control after the first ACh application (○), followed by (−)-reboxetine (□), and ACh again (●) during the second ACh application (n = 5). Note a full recovery of responses to ACh after application of 0.1–1000 μM (−)-reboxetine, suggesting the absence of any residual inhibition. (B) Results from (A) on a logarithmic scale. Increasing ACh and (−)-reboxetine concentrations (1-s pulses) were delivered every 30 s (symbols the same as in A). Note typical biphasic dose-response to ACh control (C) fitted with dual Hill equation and absence of responses to application of (−)-reboxetine. (C) Representative dose-response curves at concentrations of 0.1, 1, 10, 100, and 1000 μM ACh. Open bar above curves indicates time of ACh application. Calibration bars are 200 pA and 2 s. (D) Representative curve of application of 1000 μM (−)-reboxetine demonstrates lack of any apparent or aberrant currents after application of (−)-reboxetine. Open bar above curve represents exact timing of (−)-reboxetine application. Calibration bars are 40 pA and 2 s. The results shown are the mean (± S.E.M.) of four cells, where some error bars lie within the symbol size.

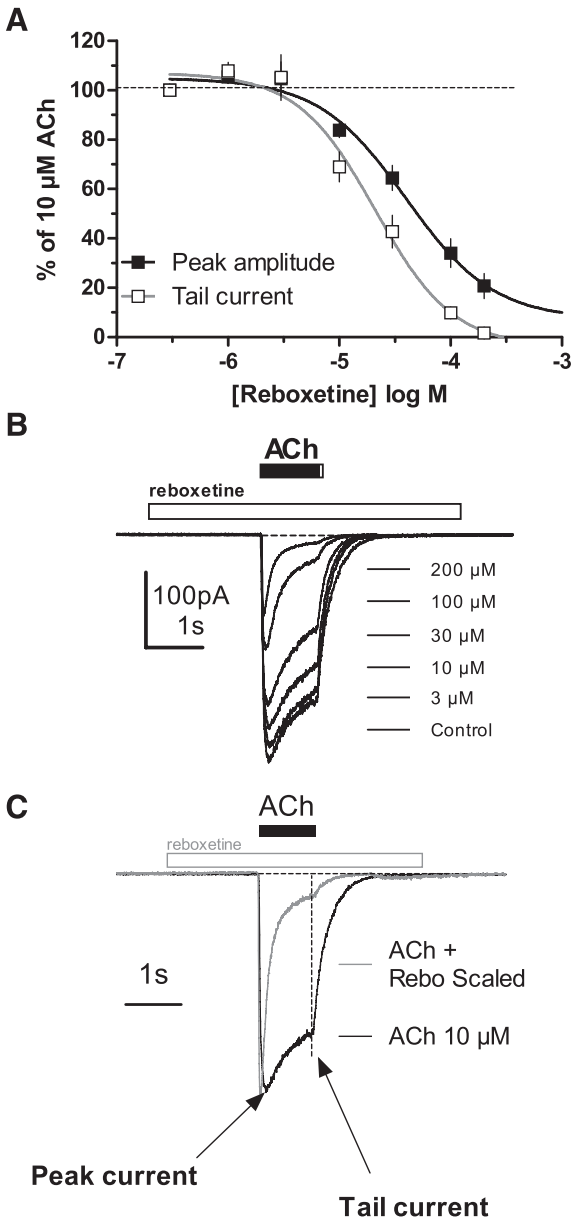

Fig. 3. Functional inhibition of h$\alpha 4\beta 2$ nAChR responses by (−)-reboxetine. (A) Full dose-response inhibition mediated by (−)-reboxetine (i.e., 3–200 μM) on the peak current amplitude (■) and tail current (□) measurements, respectively. (B) Representative examples of inhibition produced by increasing concentrations of (−)-reboxetine. Note that peak current amplitude was inhibited to a lesser extent than the tail current, leading to a profound change in current kinetics [τ values of 0.43 and 0.15 s for control and (−)-reboxetine, respectively]. Bars above the plot indicate time of application of ACh (black) and (−)-reboxetine (white), respectively. Calibration under curves is 100 pA and 1 s. (C) Scaled curves of h$\alpha 4\beta 2$ nAChR responses to ACh in the absence (control) and in the presence of (−)-reboxetine (200 μM), respectively, exemplify the profound changes in current kinetics. Vertical dashed line indicates the time point for tail current measurements. Time scale 1-s. Bars above curves show timing of ACh (black) and (−)-reboxetine (white) applications, respectively.

blocking mechanism, we used a protocol for use-dependent inhibition commonly implemented for well-known open channel blockers of nAChRs (Fedorov et al., 2009; Giniatullin et al., 2000). The protocol consisted of 10 consecutive applications of ACh at a single concentration in controls to establish a stable baseline, followed by 10 consecutive applications of the same concentration of ACh in the presence of a single concentration of (−)-reboxetine. To address recovery from inhibition (in terms of reversibility), 10 additional applications of ACh were performed at the end of the protocol. The results of these experiments are shown in Fig. 4. In the first set of experiments, we used 10 μM ACh and 1 μM (−)-reboxetine (Fig. 4A). The first coapplication of 1 μM (−)-reboxetine and ACh did not produce significant inhibition of h$\alpha 4\beta 2$ nAChR responses (~4%; $t > 0.05$; Student t test). Repetition of ACh applications in the presence of (−)-reboxetine (10 times) resulted in a modest yet significant ($t < 0.05$; one-way ANOVA) slow onset inhibition during stimulation ($\tau > 20000$ pulses). After application of 10 pulses, the amplitude of responses was inhibited by 15% ± 4%. In the second set of experiments, we used 10 μM (−)-reboxetine to evaluate the concentration dependency of this use-dependent type of inhibition. As can be seen in Fig. 4A, at this concentration, the first application of ACh in the presence of (−)-reboxetine was inhibited by 11%, whereas the last (10th application) was inhibited by 26%. Overall, one-way ANOVA showed significant differences between control applications and 1 and 10 μM (−)-reboxetine and significant differences between 1 and 10 μM applications of (−)-reboxetine ($P < 0.05$). In addition, the inhibitory action of (−)-reboxetine was readily reversible. Washout of 10 μM (−)-reboxetine resulted in fast recovery of responses to ACh with a time constant of $\tau = 1.3$ applications after applications of ACh during washout (Fig. 4A). These results suggest that (−)-reboxetine can produce a use-dependent type of inhibition of h$\alpha 4\beta 2$ nAChR function at concentrations as low as 1 μM and in a dose-dependent manner (e.g., compare 1 μM with 10 μM in Fig. 4).

TABLE 2
Binding affinity of (−)-reboxetine for the [^{3}H]imipramine binding site in the h$\alpha 4\beta 2$ nAChR ion channel

Desensitized State		Resting State	
K_i [a]	n_H [b]	K_i [a]	n_H [b]
μM		μM	
18 ± 1	0.87 ± 0.05	38 ± 3	0.77 ± 0.05

[a] K_i values were obtained in the presence of 0.1 μM (±)-epibatidine (desensitized state) or 0.1 μM κ-BTx (resting state) (Fig. 5A), according to Eq. 2.
[b] Hill coefficient.

Radioligand Binding Experiments Using h$\alpha 4\beta 2$ nAChRs in Different Conformational States. Because (−)-reboxetine inhibits h$\alpha 4\beta 2$ nAChRs by a noncompetitive mechanism and considering that a noncompetitive mechanism can be produced by a luminal interaction, the effect of (−)-reboxetine on [^{3}H]imipramine binding to h$\alpha 4\beta 2$ nAChRs in different conformational states was studied. The [^{3}H]imipramine competition binding results show that the highest concentration of (−)-reboxetine (200 μM) inhibits 75%–85% of the specific binding of [^{3}H]imipramine to the h$\alpha 4\beta 2$ nAChR ion channel (Fig. 5A), whereas the same concentration range does not inhibit [^{3}H]cytisine binding to the h$\alpha 4\beta 2$ nAChR agonist sites. This supports the view that (−)-reboxetine is not an agonist/competitive antagonist but a noncompetitive antagonist.

The observed K_i values indicate that (−)-reboxetine interacts with the [^{3}H]imipramine binding site with relatively low affinity and that it discriminates between the resting and desensitized states (Table 2). The fact that the calculated n_H values for (−)-reboxetine are close to unity (Table 2) indicates

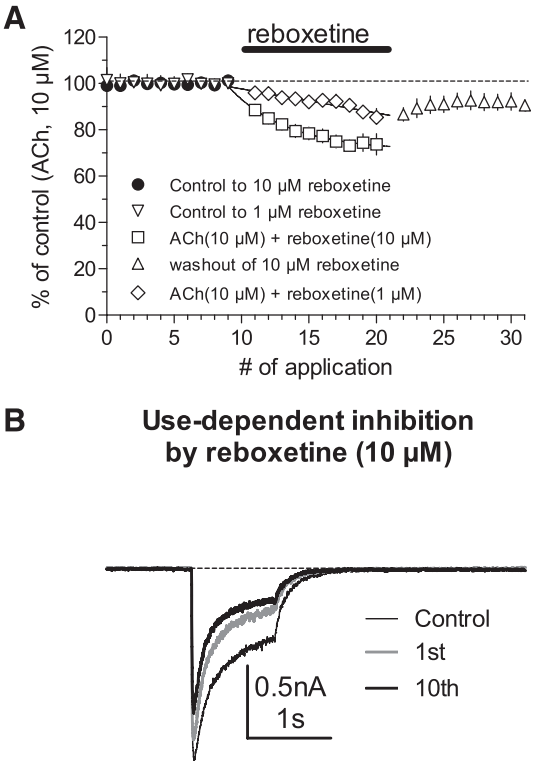

Fig. 4. Use-dependent block of responses to repetitive applications of ACh (10 μM) in the presence of 1 and 10 μM (−)-reboxetine. (A) Experimental design and results. After achieving a stable baseline with ACh in controls (▽ and ●, 5 min), ACh was applied 10 times in the presence of 1 (◇) and 10 (□) μM (−)-reboxetine (5 min). This was followed by application of 10 μM ACh alone (△, washout 5 min). (−)-Reboxetine blocked responses to ACh in a use-dependent manner, seen as a progressive increase in the extent of inhibition during repeated applications of ACh in the presence (−)-reboxetine. (−)-Reboxetine blocked ~15% and ~30% of the current with a time constant of 20,000 and 4.4 applications (1 μM and 10 μM, respectively), in a partially reversible manner.

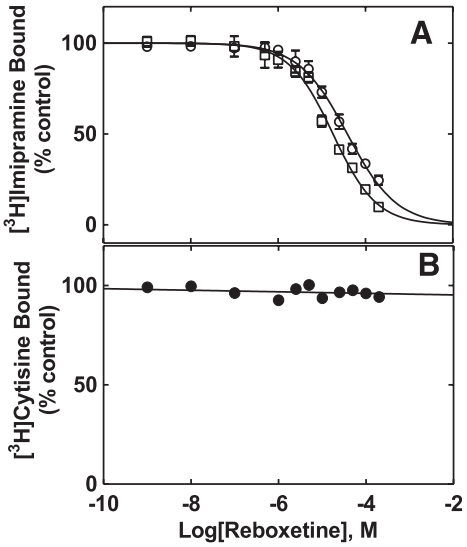

Fig. 5. Effect of (−)-reboxetine on (A) [^{3}H]imipramine and (B) [^{3}H]cytisine binding to hα4β2 nAChRs. hα4β2 nAChR membranes (1.5 mg/ml) were equilibrated (2 h) with (A) 15 nM [^{3}H]imipramine in the presence of 0.1 μM (±)-epibatidine (□) (desensitized/agonist-bound state) or 0.1 μM κ-BTx (○) (resting/κ-BTx-bound state), or with (B) 9.1 nM [^{3}H]cytisine (●), and increased concentrations of (−)-reboxetine. Nonspecific binding was determined in the presence of 100 μM imipramine (A) or 1 mM CCh (B). Each plot is the combination of three separated experiments each one performed in triplicate, where the error bars represent the S.D. values. The IC_{50} and n_H values were obtained from plots in (A) by nonlinear least-squares fit according to Eq. 1. Subsequently, the K_i values were calculated using Eq. 2. The K_i and n_H values are summarized in Table 2.

that (−)-reboxetine inhibits [^{3}H]imipramine binding in a noncooperative manner. In turn, this result suggests that (−)-reboxetine inhibits radioligand binding in a steric fashion and, consequently, that (−)-reboxetine and imipramine interact with a single binding site.

Molecular Docking of (−)-Reboxetine and Imipramine Within the hα4β2 nAChR Ion Channel. Molecular docking simulations showed that (−)-reboxetine, in the neutral and protonated states, has several putative binding sites in two different receptor regions of the hα4β2 nAChR (Table 3). One locus is situated in the ion-channel, near the cytoplasmic side between M2 residue rings 6′ and 14′ (Table 3, Fig. 6A–D). The docking experiment of imipramine gave the same result as (−)-reboxetine, where their docking sites are superposed. The same binding site within the hα4β2 nAChR ion channel was previously found (Arias et al., 2010b). Molecular dynamics simulations of these (−)-reboxetine and imipramine conformers (Fig. 7A) showed that they slightly depart from their original docked positions, but after having reached their new orientation after ~0.5 nanoseconds, imipramine remains stable for the remaining 9.5 nanosecond.

TABLE 3

hα4β2 nAChR residues involved in the binding of (−)-reboxetine to the transmembrane region and the corresponding theoretical binding affinities

For the transmembrane regions M1, M3, and M4 the total number of different residues involved in the binding of reboxetine are represented. For the transmembrane region M2, the relative position of the residue within this segment is shown.

Receptor Region	(−)-Reboxetine	M1	M2												M3	M4	Total	K_i
			6	9	10	12	13	14	15	16	18	19	21	22				μM
Bundle α4 subunit	RR N[a]	2							1						4	3	10	0.4
	RR N	2													4		6	0.7
	RR P	4													4	4	12	0.8
	RR P	4												1	6		11	1.4
	RR P	2													4		6	1.6
Ion-channel																		
	RR N[a]		2	2	2		1	1									8	0.6
	RR P		2	2	2		1	1									8	1.4

[a] Conformer with the highest affinity that is also shown in Figure 6.

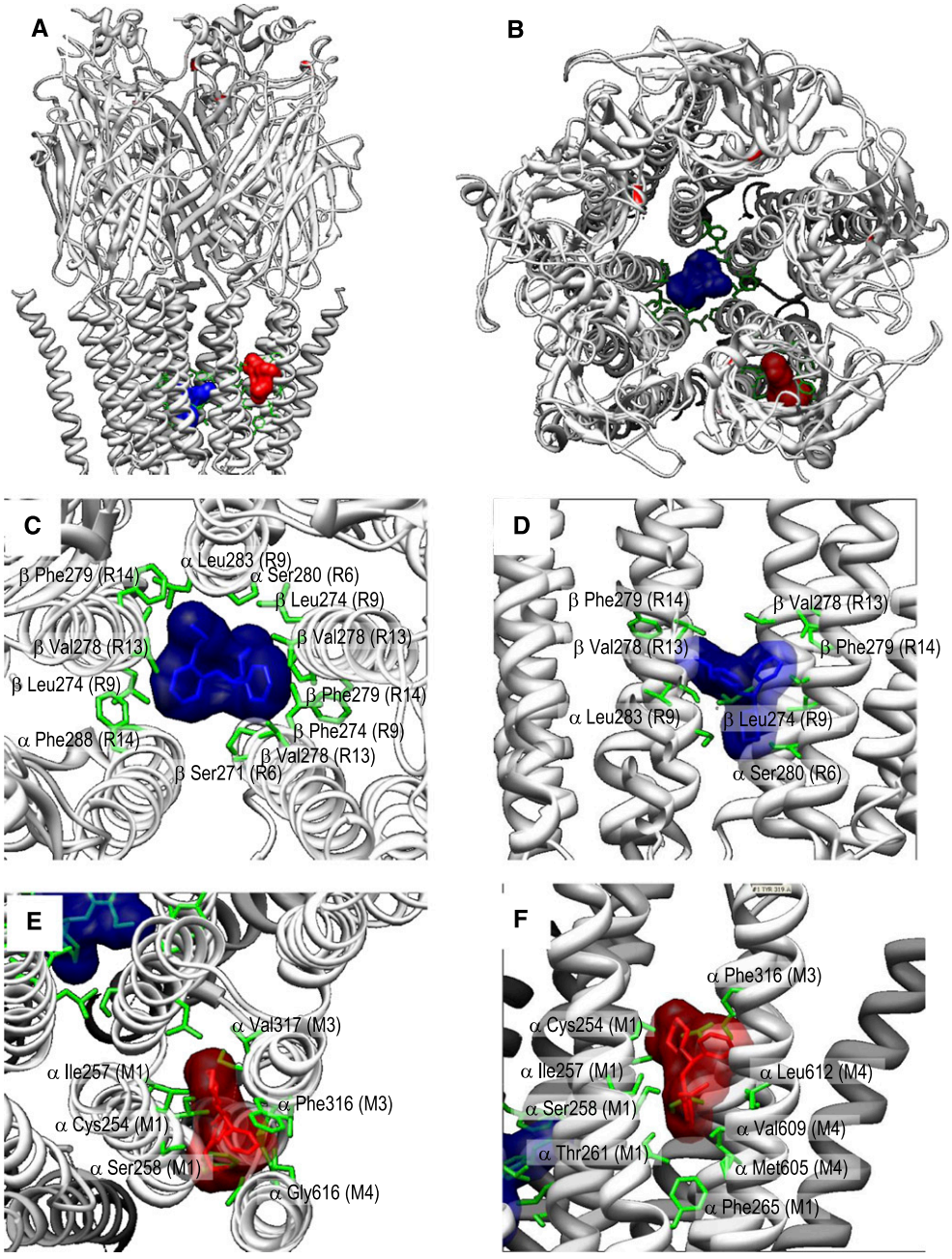

Fig. 6. Molecular interactions between (−)-reboxetine and h$\alpha 4\beta 2$ nAChR ion channel residues. (A) General side view of the h$\alpha 4\beta 2$ nAChR parallel to the membrane plane, with (−)-reboxetine docked at the imipramine binding site within the channel lumen (blue surface) and at the interior of the helix bundle of the $\alpha 4$ subunit (red surface). (B) Cytoplasmic view of the h$\alpha 4\beta 2$ nAChR with the same conformers as in (A). (C) Detailed cytoplasmic view of (−)-reboxetine (blue surface) docked at the imipramine binding site. (D) Detailed side view parallel to the membrane plane of (−)-reboxetine (blue surface) docked at the imipramine binding site. (E) Detailed cytoplasmic view of (−)-reboxetine (red surface) docked at the α-helix bundle. (F) Detailed side view parallel to the membrane plane of (−)-reboxetine (red surface) docked at the α-helix bundle. M1, M3, and M4 denote residues belonging to the corresponding transmembrane regions. R denotes the ring number of the M2 transmembrane segment.

On the other hand, (−)-reboxetine has a greater mobility from this final site. Thus, despite the fact that (−)-reboxetine binds to the same locus as imipramine, its binding is less stable. In both cases, these molecules completely block the ion channel.

The other locus where both (−)-reboxetine and imipramine bind is within the $\alpha 4$ subunit transmembrane helix bundle. At this position these drugs do not block the channel, but they can presumably alter the luminal structure of the channel, decreasing ion flux. In this case, molecular dynamics show that imipramine also changes slightly from its original docking site (as determined by the docking simulation) and maintains the new orientation without any major deviation. On the other hand, (−)-reboxetine deviates more from the original docking site, but it remains there in a more stable way than in the ion channel lumen. In this regard, it seems that (−)-reboxetine might allosterically promote changes in the channel properties with more potency, including desensitization, than would a direct block of the channel.

Discussion

The inhibitory activity of reboxetine on nAChRs (Arias et al., 2006; Miller et al., 2002) might be relevant to the observed preclinical and clinical actions elicited by this nontricyclic SNRI (Andreasen et al., 2011; Hajos et al., 2004; Rauhut et al., 2002). In this regard, the interaction of (−)-reboxetine with the h$\alpha 4\beta 2$ nAChR in different conformational states was characterized. To this end, functional and structural approaches were used, including radioligand binding assays, Ca^{2+} influx and patch-clamp methods, and molecular docking and dynamics studies.

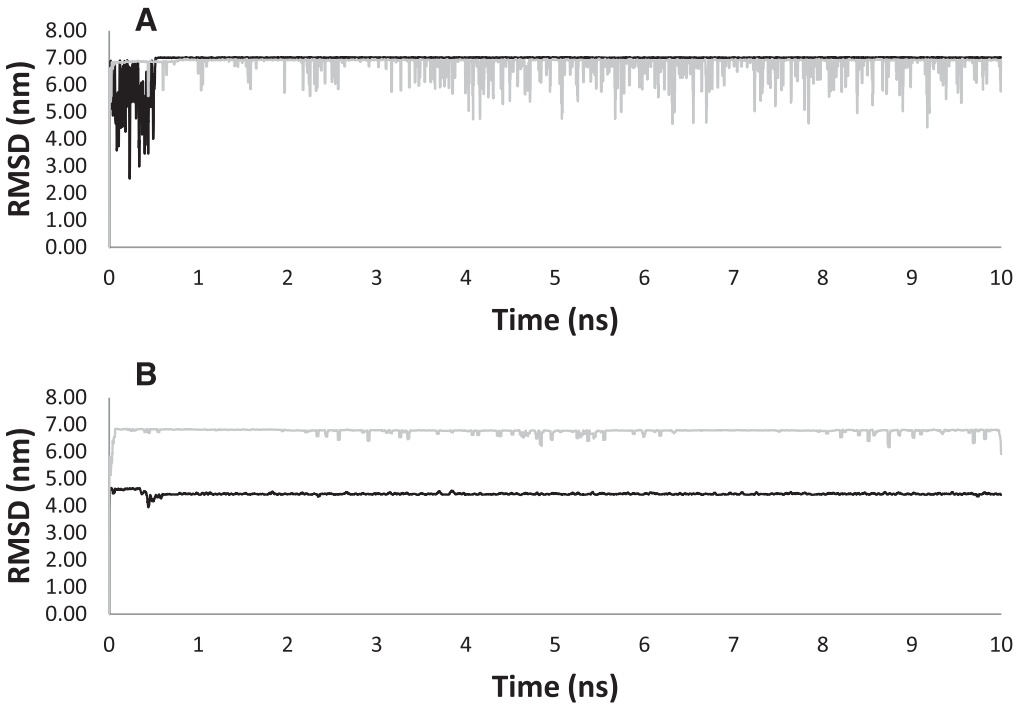

Fig. 7. Molecular dynamics of (−)-reboxetine and imipramine binding to the hα4β2 nAChR. (A) RMSD values of (−)-reboxetine (light gray line) and imipramine (black line) of a 10-ns dynamics simulation performed at their docking sites within the (A) hα4β2 nAChR ion channel and the (B) α4-subunit transmembrane helix bundle.

To determine the effect of (−)-reboxetine on (±)-epibatidine-activated Ca^{2+} influx in HEK293-hα4β2 cells, a preincubation protocol was used (Fig. 1). The results indicate that (−)-reboxetine inhibits hα4β2 nAChRs with relatively lower potency (Table 1) than that for human muscle AChRs (~2–4 μM; paper in preparation). To our knowledge, this is the first time that the inhibitory potency of (−)-reboxetine for hα4β2 nAChRs has been demonstrated. Of interest, reboxetine was found to inhibit $^{86}Rb^{+}$ efflux from thalamic synaptosomes containing primarily α4β2* nAChRs with IC_{50} of 0.65 μM (Miller et al., 2002). The observed large difference for the inhibitory potencies on the α4β2* nAChRs is commonly attributed to intrinsic methodological differences in assay conditions regarding direct (electrophysiology) versus indirect (fluorescence-based) type of measurements and properties of signal carriers ($^{86}Rb^{+}$ versus fluorescent dye).

To confirm and expand the results from the fluorescence-based screening assays, we also investigated the excitatory and/or inhibitory actions of (−)-reboxetine on hα4β2 nAChRs function with use of electrophysiology-based approaches on SHEP1-hα4β2 cells, which provide direct measurements of ion flow through the ion channel. First, we found that applications of (−)-reboxetine over a wide concentration range (0.1–1000 μM) did not produce any measurable currents. We did not find any hint of transient and/or aberrant currents, which would be apparent in cases of a mixture of excitatory and inhibitory action at certain concentrations. This suggests the following possibilities: (1) (−)-reboxetine does not interact with the orthosteric site of the hα4β2 nAChR in an agonist-like fashion, (2) it interacts with the orthosteric sites in a competitive antagonist fashion, and (3) the potency of the inhibitory action of (−)-reboxetine greatly exceeds (leftward shift) the potency of agonist-like actions. To address these possibilities, we first determined the inhibitory action of (−)-reboxetine and found that (−)-reboxetine appeared to be an inhibitor of hα4β2 nAChR function. Of interest, (−)-reboxetine exhibited a different magnitude of inhibition that was dependent on the time and exposure of the open channel state during applications of ACh with (−)-reboxetine. The amplitude of the peak current showed an IC_{50} of ~40 μM, whereas the steady-state portion of the current (i.e., the tail current) showed an IC_{50} of ~21 μM (Table 1). This pharmacological pattern resembles that for the recently described AMPA receptor blockers (Zaitsev et al., 2011). Consistently, the difference in potencies was associated with significant changes in the current kinetics of ACh-induced activation of hα4β2 nAChRs, which were found to be 3.2-fold faster in the presence of 200 μM (−)-reboxetine (τ = 0.471 s versus τ = 0.147 s). There are two main types of inhibition of nAChR function (competitive and noncompetitive), based on the affinity of an antagonist for the nAChR orthosteric sites. These results suggested that at low concentrations, the inhibitory action of (−)-reboxetine was primarily mediated by a noncompetitive type of inhibition, presumably via open-channel block.

To confirm the potential open-channel blocking mechanism, we investigated the extent of use-dependent inhibition, which represents a well-known feature of open-channel blockers of nAChRs (Fedorov et al., 2009; Giniatullin et al., 2000). We found that (−)-reboxetine was capable of producing small yet significant use-dependent inhibition in a concentration-dependent manner (1 μM and 10 μM). Of importance, even at the lowest concentrations of (−)-reboxetine used (1 μM), we were able to demonstrate significant use-dependent inhibition (by 15%) during only 10 consecutive agonist applications. It is known that use-dependent inhibition is dependent on the

number of uses (i.e., the number of openings and/or the time of exposure of channels in the open state to the antagonist). The number of potential opening events in the brain is quite large, far exceeding the 10 applications used in our model (due to channel flickering and opening of channels as a result of spontaneous and/or evoked endogenous transmitter release). Thus, it could be speculated that the continuous presence of a pharmacologically relevant concentration of (−)-reboxetine (~1 μM) in the system, the noncompetitive, use-dependent inhibitory action described here, would dominate other types of potential interactions. This also calls into question the mechanistic differentiation between functional desensitization and open-channel blocked states of receptors. In this regard, although our results suggest that (−)-reboxetine at low concentrations mainly acts via an open channel blocking mechanism, (−)-reboxetine–induced nAChR desensitization cannot be completely ruled out.

Because the inhibitory action of (−)-reboxetine on agonist-induced h$\alpha4\beta2$ nAChR activation is mediated by a noncompetitive mechanism (see Figs. 1B and 2B), we tested whether (−)-reboxetine binds to the nAChR lumen by [^{3}H]imipramine competition binding experiments. The results indicate that (−)-reboxetine binds with ~2-fold higher affinity to the desensitized h$\alpha4\beta2$ nAChR, compared with the resting nAChR (see Table 2). Considering that the n_H values from these competition experiments are close to unity, (−)-reboxetine may be interacting with the imipramine binding site in a steric fashion. Consistent with these results, (−)-reboxetine does not bind to the h$\alpha4\beta2$ nAChR agonist sites (see Fig. 5B). Previous experiments using rat whole-brain membranes also showed that reboxetine binds with very low affinity to the nAChR agonist sites (Miller et al., 2002). Previous results from our laboratory indicate that tricyclic antidepressants and selective serotonin reuptake inhibitors (Arias et al., 2010b; Arias, 2010) bind to overlapping sites in a domain formed between the serine (position 6′) and valine (position 13′) rings of the h$\alpha4\beta2$ nAChR ion channel. In this regard, our radioligand binding (Table 2) and docking (see Fig. 6) results support the view that (−)-reboxetine also binds to the same binding domain as that for these structurally different antidepressants.

The plasma concentration of (−)-reboxetine in patients receiving long-term treatment (6 months) can reach values as high as ~1 μM (Ohman et al., 2003). New insights into the potential use-dependent mechanism of inhibition demonstrated in the present study using electrophysiology-based assays suggest that (−)-reboxetine at concentrations as low as 1 μM is capable of producing small, yet significant, concentration and use-dependent inhibition of h$\alpha4\beta2$ nAChR function. Although the clinical concentration of reboxetine and magnitude of effect was found not within physiologically relevant margins, our results suggest that (−)-reboxetine can inhibit h$\alpha4\beta2$ nAChRs in a clinically significant concentration range by blocking the $\alpha4\beta2$ nAChR ion channel through the interaction with the tricyclic antidepressant locus.

Our results support the idea that the clinical action of reboxetine is mediated, at least partially, by a noncompetitive inhibitory (blocking) mechanism on h$\alpha4\beta2$ nAChRs. Inhibitory mechanisms have also been reported for tricyclic antidepressants, bupropion, and selective serotonin reuptake inhibitors in muscle- (Arias et al., 2009; Arias et al., 2010a; Gumilar et al., 2003; Lopez-Valdes and Garcia-Colunga, 2001) and neuronal-type nAChRs (Arias et al., 2010b; Arias et al., 2010c; Arias et al., 2010d; Gumilar and Bouzat, 2008; Lopez-Valdes and Garcia-Colunga, 2001). This evidence suggests that there is a basic mechanistic motif for structurally different antidepressants mediating the inhibition of distinct nAChRs.

Authorship Contributions

Participated in research design: Arias, Fedorov, Benson, Gatto, Lippiello, Feuerbach, Ortells.

Conducted experiments: Arias, Fedorov, Benson, Feuerbach, Ortells.

Contributed new reagents or analytic tools: Fedorov, Gatto.

Performed data analysis: Arias, Fedorov, Benson, Lippiello, Feuerbach, Ortells.

Wrote or contributed to the writing of the manuscript: Arias, Fedorov, Benson, Gatto, Lippiello, Feuerbach, Ortells.

References

Albuquerque EX, Pereira EF, Alkondon M, and Rogers SW (2009) Mammalian nicotinic acetylcholine receptors: from structure to function. *Physiol Rev* **89**: 73–120.

Andreasen JT, Nielsen EO, Christensen JK, Olsen GM, Peters D, Mirza NR, and Redrobe JP (2011) Subtype-selective nicotinic acetylcholine receptor agonists enhance the responsiveness to citalopram and reboxetine in the mouse forced swim test. *J Psychopharmacol* **25**:1347–1356.

Arias HR (2010) Positive and negative modulation of nicotinic receptors. *Adv Protein Chem Struct Biol* **80**:153–203.

Arias HR, Bhumireddy P, and Bouzat C (2006) Molecular mechanisms and binding site locations for noncompetitive antagonists of nicotinic acetylcholine receptors. *Int J Biochem Cell Biol* **38**:1254–1276.

Arias HR, Feuerbach D, Bhumireddy P, and Ortells MO (2010a) Inhibitory mechanisms and binding site location for serotonin selective reuptake inhibitors on nicotinic acetylcholine receptors. *Int J Biochem Cell Biol* **42**:712–724.

Arias HR, Feuerbach D, Targowska-Duda KM, Russell M, and Jozwiak K (2010b) Interaction of selective serotonin reuptake inhibitors with neuronal nicotinic acetylcholine receptors. *Biochemistry* **49**:5734–5742.

Arias HR, Gumilar F, Rosenberg A, Targowska-Duda KM, Feuerbach D, Jozwiak K, Moaddel R, Wainer IW, and Bouzat C (2009) Interaction of bupropion with muscle-type nicotinic acetylcholine receptors in different conformational states. *Biochemistry* **48**:4506–4518.

Arias HR, Rosenberg A, Targowska-Duda KM, Feuerbach D, Jozwiak K, Moaddel R, and Wainer IW (2010c) Tricyclic antidepressants and mecamylamine bind to different sites in the human alpha4beta2 nicotinic receptor ion channel. *Int J Biochem Cell Biol* **42**:1007–1018.

Arias HR, Targowska-Duda KM, Feuerbach D, Sullivan CJ, Maciejewski R, and Jozwiak K (2010d) Different interaction between tricyclic antidepressants and mecamylamine with the human alpha3beta4 nicotinic acetylcholine receptor ion channel. *Neurochem Int* **56**:642–649.

Brooks BR, Brooks CL, 3rd, and Mackerell AD, Jr, et al. (2009) CHARMM: the biomolecular simulation program. *J Comput Chem* **30**:1545–1614.

Cheng Y and Prusoff WH (1973) Relationship between the inhibition constant (K1) and the concentration of inhibitor which causes 50 per cent inhibition (I50) of an enzymatic reaction. *Biochem Pharmacol* **22**:3099–3108.

Fedorov NB, Benson LC, Graef J, Lippiello PM, and Bencherif M (2009) Differential pharmacologies of mecamylamine enantiomers: positive allosteric modulation and noncompetitive inhibition. *J Pharmacol Exp Ther* **328**:525–532.

Gerzanich V, Peng X, Wang F, Wells G, Anand R, Fletcher S, and Lindstrom J (1995) Comparative pharmacology of epibatidine: a potent agonist for neuronal nicotinic acetylcholine receptors. *Mol Pharmacol* **48**:774–782.

Giniatullin RA, Sokolova EM, Di Angelantonio S, Skorinkin A, Talantova MV, and Nistri A (2000) Rapid relief of block by mecamylamine of neuronal nicotinic acetylcholine receptors of rat chromaffin cells in vitro: an electrophysiological and modeling study. *Mol Pharmacol* **58**:778–787.

Gorman JM and Kent JM (1999) SSRIs and SNRIs: broad spectrum of efficacy beyond major depression. *J Clin Psych* **60**(Suppl 4):33–38.

Grubmüller H, Heymann B, and Tavan P (1996) Ligand binding: molecular mechanics calculation of the streptavidin-biotin rupture force. *Science* **271**:997–999.

Gumilar F, Arias HR, Spitzmaul G, and Bouzat C (2003) Molecular mechanisms of inhibition of nicotinic acetylcholine receptors by tricyclic antidepressants. *Neuropharmacology* **45**:964–976.

Gumilar F and Bouzat C (2008) Tricyclic antidepressants inhibit homomeric Cys-loop receptors by acting at different conformational states. *Eur J Pharmacol* **584**:30–39.

Hajós M, Fleishaker JC, Filipiak-Reisner JK, Brown MT, and Wong EH (2004) The selective norepinephrine reuptake inhibitor antidepressant reboxetine: pharmacological and clinical profile. *CNS Drug Rev* **10**:23–44.

Hennings EC, Kiss JP, De Oliveira K, Toth PT, and Vizi ES (1999) Nicotinic acetylcholine receptor antagonistic activity of monoamine uptake blockers in rat hippocampal slices. *J Neurochem* **73**:1043–1050.

Izaguirre V, Fernández-Fernández JM, Ceña V, and González-García C (1997) Tricyclic antidepressants block cholinergic nicotinic receptors and ATP secretion in bovine chromaffin cells. *FEBS Lett* **418**:39–42.

Liu Q, Yu KW, Chang YC, Lukas RJ, and Wu J (2008) Agonist-induced hump current production in heterologously-expressed human alpha4beta2-nicotinic acetylcholine receptors. *Acta Pharmacol Sin* **29**:305–319.
López-Valdés HE and García-Colunga J (2001) Antagonism of nicotinic acetylcholine receptors by inhibitors of monoamine uptake. *Mol Psychiatry* **6**:511–519.
Mathur A, Shankaracharya, and Vidyarthi AS (2011) SWIFT MODELLER: a Java based GUI for molecular modeling. *J Mol Model* **17**:2601–2607.
Michelmore S, Croskery K, Nozulak J, Hoyer D, Longato R, Weber A, Bouhelal R, and Feuerbach D (2002) Study of the calcium dynamics of the human alpha4beta2, alpha3beta4 and alpha1beta1gammadelta nicotinic acetylcholine receptors. *Naunyn Schmiedebergs Arch Pharmacol* **366**:235–245.
Miller DK, Wong EH, Chesnut MD, and Dwoskin LP (2002) Reboxetine: functional inhibition of monoamine transporters and nicotinic acetylcholine receptors. *J Pharmacol Exp Ther* **302**:687–695.
Miyazawa A, Fujiyoshi Y, and Unwin N (2003) Structure and gating mechanism of the acetylcholine receptor pore. *Nature* **423**:949–955.
Moore MA and McCarthy MP (1995) Snake venom toxins, unlike smaller antagonists, appear to stabilize a resting state conformation of the nicotinic acetylcholine receptor. *Biochim Biophys Acta* **1235**:336–342.
Ohman D, Cherma MD, Norlander B, and Bengtsson F (2003) Determination of serum reboxetine enantiomers in patients on chronic medication with racemic reboxetine. *Ther Drug Monit* **25**:174–182.
Paterson NE, Semenova S, and Markou A (2008) The effects of chronic versus acute desipramine on nicotine withdrawal and nicotine self-administration in the rat. *Psychopharmacology (Berl)* **198**:351–362.
Pedretti A, Villa L, and Vistoli G (2004) VEGA—an open platform to develop chemo-bio-informatics applications, using plug-in architecture and script programming. *J Comput Aided Mol Des* **18**:167–173.
Phillips JC, Braun R, Wang W, Gumbart J, Tajkhorshid E, Villa E, Chipot C, Skeel RD, Kalé L, and Schulten K (2005) Scalable molecular dynamics with NAMD. *J Comput Chem* **26**:1781–1802.
Picciotto MR, Brunzell DH, and Caldarone BJ (2002) Effect of nicotine and nicotinic receptors on anxiety and depression. *Neuroreport* **13**:1097–1106.
Rana B, McMorn SO, Reeve HL, Wyatt CN, Vaughan PF, and Peers C (1993) Inhibition of neuronal nicotinic acetylcholine receptors by imipramine and desipramine. *Eur J Pharmacol* **250**:247–251.
Rauhut AS, Mullins SN, Dwoskin LP, and Bardo MT (2002) Reboxetine: attenuation of intravenous nicotine self-administration in rats. *J Pharmacol Exp Ther* **303**: 664–672.
Sali A and Blundell TL (1993) Comparative protein modelling by satisfaction of spatial restraints. *J Mol Biol* **234**:779–815.
Shytle RD, Silver AA, Lukas RJ, Newman MB, Sheehan DV, and Sanberg PR (2002) Nicotinic acetylcholine receptors as targets for antidepressants. *Mol Psychiatry* **7**: 525–535.
Unwin N (2005) Refined structure of the nicotinic acetylcholine receptor at 4A resolution. *J Mol Biol* **346**:967–989.
Zaitsev AV, Kim KK, Fedorova IM, Dorofeeva NA, Magazanik LG, and Tikhonov DB (2011) Specific mechanism of use-dependent channel block of calcium-permeable AMPA receptors provides activity-dependent inhibition of glutamatergic neurotransmission. *J Physiol* **589**:1587–1601.

Address correspondence to: Dr. Nikolai Fedorov, Preclinical Research, Targacept, Inc., 200 East First Street, #300, Winston Salem, NC, 27101. E-mail: nikolai.fedorov@targacept.com